

## Turn Scanning: Experimental and Theoretical Approaches to the Role of Turns

Carl Frieden, Enoch S. Huang, and Jay W. Ponder

### 1. Introduction

The mechanism that enables a protein to fold to its correct three-dimensional conformation—given only the information available from its sequence—has been a matter of intense investigation since Anfinsen's classical experiment on the refolding of ribonuclease almost 40 years ago (*1*). The importance of turn sequences in the kinetic and thermodynamic aspects of protein folding remains a controversial point, although their role—especially for  $\alpha$ -turns—has been regarded as significant (i.e., *2–10*). What role, if any, do turn sequences play in determining the native structures of proteins? For the experimentalist, this question is usually rephrased as: to what extent can substitution, insertion, and deletion be tolerated at turn positions before kinetic and/or thermodynamic properties are affected? It is indeed surprising how few experimental studies have been performed to carefully investigate the role of turns. To the theoretician, this question of the importance of turns revolves around the ability of computational studies to attempt to determine the propensity of isolated small peptides, as well as larger structures, to form turns. While much research has been conducted in this field, even here the answers remain uncertain.

From: *Methods in Molecular Biology*, vol. 168: *Protein Structure, Stability, and Folding*  
Edited by: K. P. Murphy © Humana Press Inc., Totowa, NJ

In this chapter, we draw on both experimental and theoretical results in an attempt to answer the question. Part of the debate in the experimental literature concerns the issue of whether turns play an active or passive role in protein folding. If we accept the theory that isolated turn sequences may be intrinsically unstable, it may be tempting to conclude that turns will play only a passive role in protein folding. While this view may have value for very small peptides, it can be overly simplistic for at least two reasons. First, there is evidence that sequence-specific intraturn side-chain interactions can stabilize turn structures. Second, early, nonspecific stages of protein folding—such as a generalized hydrophobic collapse phase—could supply additional constraints that might allow turn sequences to act as nucleation sites for a more ordered structure. For example, hydrophobic interactions within a folding  $\beta$ -hairpin may restrict the range of extended structures available to the included turn and disrupt the turn-water entropic effects favoring extended structures.

Here we present the use of turn scanning as an experimental method for assessing the role of turns in the folding process. Turn scanning—in analogy to methods such as alanine scanning—is the systematic replacement of residues in a turn followed by an examination of the consequences of the change in terms of rates of folding or unfolding, stability to denaturing conditions, and structural changes using various biophysical techniques. An obvious candidate for replacement would be glycine. Replacing this residue in a turn may lead to a change in the turn type. Similarly, replacing a residue with glycine may lead to greater flexibility within the turn. Another obvious candidate is proline, involving either an insertion or a replacement. Changes should certainly not be limited to these two residues. Substitutions between hydrophobic and hydrophilic residues, or between residues with a large and small side chains, are equally valuable. For example, replacing a leucine in one of the turns of the fatty-acid-binding protein was found to lead to a very unstable protein that folded rapidly to an intermediate state (*II*). However, one must be careful with the results. The permissive sub-

stitution of native-turn residues does not necessarily imply a passive role for the turn. The native-turn sequence may in fact actively drive or stabilize hairpin formation more than other segments of similar length, but in the absence of the native sequence, other interatomic forces may be sufficiently strong to drive folding, making the mutated sequence a turn by default. This point is made eloquently in the work of DeGrado and colleagues (*12*). By the same logic, extreme intolerance to substitution does not necessarily mean that the native sequence plays an active role in folding. For example, the substitution of another residue for glycine in a turn may abolish folding because of the steric clashes resulting from the presence of a beta-carbon. Does the glycine actively direct turn formation, or is its presence merely required, as it is the only amino acid that does not destabilize the requisite local conformation? The point is to caution that equilibrium and kinetic experiments should be coupled with other biophysical techniques to resolve the issue of the importance of turn structure in the folding process.

## ***2. Kinetic Evidence for the Importance of Turn Formation in the Folding Process***

### ***2.1. Experimental Results from Model Systems***

Researchers have generally chosen peptides or small proteins as model systems. In either case, the rationale is that they exhibit simple two-state behavior—i.e., the protein is either in an unfolded or folded state with no populated intermediate state. While in reality, many systems are no longer two-state—especially when investigated using site-directed mutagenesis to perturb the folding process—the results from these model systems provide evidence for the importance of turn formation in protein folding.

### ***2.2. Peptide Model Systems***

A logical approach to measure the rate of turn formation is to utilize peptides with a natural tendency to form  $\beta$ -turns, and then

perturb the system by using different amino acids in specific positions. Several investigators have done this. De Alba et al. (*13*) have constructed model linear peptides in which the only difference was in the putative turn region. Their results clearly demonstrated that the turn residue sequence determined the turn conformation, and thereby other features such as interstrand pairing and hydrogen bonding. Munoz et al. (*14*) have studied the kinetics of one peptide (16 aa) that reflected the  $\beta$ -hairpin from protein G B1 using laser temperature-jump and found that folding of the hairpin occurs in 6 ns at room temperature. This chapter is followed by a statistical mechanical model for  $\beta$ -hairpin kinetics (*15*) in which the authors attempt to predict the kinetic properties of other similar peptides. The results of the work of Serrano and colleagues are also particularly pertinent. Blanco and Serrano—using circular dichroism and NMR (nuclear magnetic resonance)—have examined the solution structure of the isolated fragments 1–20 ( $\beta$ -hairpin), 21–40 ( $\beta$ -helix), and 41–56 ( $\beta$ -hairpin), corresponding to all the secondary-structure elements of the protein G B1 domain. Turn-like folded structures were detected in water, although they were poorly populated (*16*). Ramirez-Alvarado et al. (*17*) have designed a 12-residue model peptide that folded into a monomeric  $\beta$ -sheet. Substitution of strand residues by alanine led to the loss of the hairpin structure, demonstrating the importance of side-chain interactions between the strands. Mutations in the turn of the same peptide (*18*) showed that changing the central residue of a type I  $\beta$ -turn affected stability. These and other experiments from this laboratory (*7*) led Blanco et al. (*19*) to emphasize the importance of residues within and near the turn in stabilizing  $\beta$ -hairpin structures. It is interesting that umbrella sampling with the CHARMM force field and ACE implicit solvation model has been used to estimate the stability of the peptide examined by Ramirez-Alvarado et al. (*18*). These calculations (*20*) predicted a 38% content of hairpin structure at room temperature with less than 1% helical content, and the remainder in various unfolded states. There appears to be a much lower barrier for this transition between the hairpin and unfolded states than for the corresponding helix-coil transition.

There is little doubt that changing residues within turns of model peptides affects stability and conformation, as many studies have now shown. However, only a few of these studies have been directed toward the effect of the change on the kinetic properties. This may be a consequence of the fact that very rapid techniques (i.e.,  $\mu$ s or shorter) are not generally available. Clearly, such experiments are essential for evaluating the role of turns in the kinetics of folding. Theoretical results may thus become complementary to experimental results—as the former tries to extend simulations to longer times, while the latter attempts to determine events that occur at early times.

### **2.3. Protein Model Systems**

The intestinal fatty-acid binding protein is an excellent model for folding studies because it is almost entirely  $\beta$ -sheet, and 7 of the 8 turns between  $\beta$ -strands include a glycine residue. Kim and Frieden (21) carefully examined the effect of mutations in turns on the stability and refolding of this protein by mutating each of these glycines to valine. In some cases, the mutation had little or no effect on folding or stability, while in other cases the effect was dramatic. Specifically, mutations in type II turns—while very destabilizing—did not markedly affect the rate of structure formation, while the mutation of a glycine to valine in the turn between the two last  $\beta$ -strands of IFABP slowed the rate of folding by at least 100-fold. Furthermore, the refolding rate constant for this mutant was observed to be essentially independent of the final denaturant concentration (21). Random mutagenesis in another turn (between the D and E strands) led to the conclusion that a leucine residue was critical for formation of the final stable structure and perhaps for an initial nucleation step as well (11). These experiments represent one of the first attempts to critically evaluate the role of different turns in the overall folding process.

While almost all of the turn mutants of the fatty-acid binding protein examined were able to fold and bind fatty acid, a very different observation was made for plastocyanin. Ybe and Hecht (22) found that the vast majority (92 of 98) of four-residue turn mutants of this

protein apparently could not fold into the native  $\beta$ -barrel topology. Results of Gu et al. (23) also highlighted severe sequence constraints in two  $\beta$ -turns of peptostreptococcal protein L. Because their mutants were presented on a phage display system, enumeration and sequencing of all the mutants was not possible. Nevertheless, biopanning against the immunoglobulin G (IgG) binding activity of protein L showed that less than 0.1% of the phage from the two libraries (one for each turn that was mutagenized) were recovered.

Schonbrunner et al. (9) have presented evidence that hairpins may serve as initiation sites for  $\beta$ -sheet formation. These authors used the small (74 aa)  $\beta$ -sheet protein tendaminstat that contains two disulfide bonds, one of which connects the ends of a  $\beta$ -hairpin. Using site-directed mutagenesis of one of these cysteines, they found that unfolding is greatly enhanced, but with a greatly reduced effect on the refolding rate. Using a Fersht analysis ( $k_{-1} > 1$ ), they concluded—based on thermodynamic and kinetic arguments—that formation of the hairpin turn is the rate-limiting step in the refolding process.

Some studies suggest that turns connecting alpha-helices are rather robust with respect to mutation. In the early work by Hecht and colleagues (24), a three-residue turn in the four-helix bundle cytochrome b-562 was randomized to 31 unique sequences, and all the mutants folded correctly. Subsequent experiments on the four-helical Rop dimer provide corroborating evidence. In one study, Regan and colleagues (25) changed one of the two residues (Asp30) involved in the tight turn between the two helices of the monomer into every other amino acid without misfolding the protein. In another study, Cesareni and colleagues (26) mutated three residues semirandomly in the turn region of the Rop monomer (residues 30 to 32), and found only three mutants out of a possible 380 that failed to fold correctly. Yet substitution of a proline for alanine in the turn caused drastic changes (27). Finally, MacBeath et al. (28) conducted a highly comprehensive randomization of an interhelical turn in *Escherichia coli* chorismate mutase—also a four-helix bundle. The authors reported that more than 63% of tripeptide sequences can functionally substitute for the native-turn sequence in this enzyme.

Nagi et al. (29), examining the folding pathway of the four-helix bundle protein, Rop, replaced the wild-type two-residue loop between helical regions with a series of polyglycine linkers of increasing length. They then investigated the kinetics of unfolding and refolding, and observed a large dependence of rates as the loop length increased from 2 to 4, but little dependence beyond that. They suggested that the results were consistent with lowering the energy barrier of the transition state, and that this type of experiment can test potential folding models. Similar experiments on changing loop lengths have been reported by Viguera and Serrano (30) and by Ladurner and Fersht (31). The results of this type of experiment may reveal the importance of turn formation relative to interactions between structural units on either side of the turn.

Currently, there is a growing database that describes the altered stability of proteins with mutated turns. The recurrent theme is that mutations in loops generally reduce the thermodynamic stability of the folded state (11,12,23,32,33) although exceptions do exist (25). Consequently, misfolded mutants may correspond to those whose altered turn residues—if forced to assume the native conformation—would exact a thermodynamic penalty exceeding that of the scaffold's overall stability (12). This line of reasoning thus offers two factors for the differential sensitivity towards turn mutation: 1) the inherent stability of the scaffold, and 2) the energetic demands upon the turn in question.

### **3. How to Relate Changes in Kinetic Parameters to the Importance of Turn Formation in the Folding Process**

Much of the interpretation of the effect of mutations on rate constants of unfolding or refolding in the presence of chemical denaturants has been based on a simple two-state model, N  $\rightleftharpoons$  U. Jackson and Fersht (34) have discussed chevron plots (i.e., plots of the log of the relaxation rate or rate constant as a function of the denaturant concentration) for the two-state model. The results of mutagenesis of a wild-type protein can affect these plots in at least three ways: an

equilibrium mutation in which both folding and unfolding rate constants are affected equally with no change in stability; a kinetic mutation in which one of the rate constants is changed, along with a change in stability, but the other is not; or a mixed equilibrium-kinetic effect. Fersht and colleagues (35) have developed the use of the quantity  $\Delta G_{I-D} / \Delta G_{N-D}$  to determine the mutations effect on processes before or after the transition state for a folding pathway that includes an intermediate. In this calculation, this ratio is the change in free energy on mutation relative to the overall free energy of folding. If  $\Delta G_{I-D} / \Delta G_{N-D} = 1$  or  $0$ , the interpretation is reasonably straightforward, reflecting whether the transition state is perturbed by mutation to the same extent as the denatured state ( $\Delta G_{I-D} / \Delta G_{N-D} = 1$ ) or the native state ( $\Delta G_{I-D} / \Delta G_{N-D} = 0$ ). Unfortunately, the actual interpretation is more difficult. First, many systems show more than one rate in the folding process, suggesting the presence of intermediates. Frequently, there is a burst too rapid to measure by normal stopped-flow techniques. Second, one must consider what the rates are actually measuring. For example, using changes in fluorescence (or A or circular dichroism, the most common methods of following folding or unfolding), it is usually unclear what the contribution of intermediate states to the observed change actually is. Third, there is the issue of whether observed phases represent intermediates or off-pathway forms. Fourth, the log of the rate constant is not always a linear function of the denaturant concentration (i.e., the chevron plot is nonlinear). Certainly, proline isomerization will affect this linearity, but such observations can be made even for a protein that does not contain proline (21). The issue of the nonlinearity in chevron plots unrelated to proline isomerization has been discussed by other authors (36,37). From this perspective, it is easy to see why investigators want to use model peptides. For proteins, however, all is not lost. Despite these complexities, some generalizations are possible. For example, if the amplitude of a refolding burst phase is decreased by the mutation, it is likely an early step that is affected. Similarly, if the burst phase is unaffected, a late step may be responsible. But there are caveats for even this simple interpretation. Thus, for com-

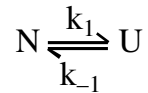


parison of a mutant to wild-type, one must know the midpoint and the degree of cooperativity of the equilibrium denaturation curve. A loss in cooperativity (the  $m$  value of the 6-term equation that describes equilibrium denaturation measurements [38]) suggests increased concentrations of one or more intermediates as a result of the increase in the rate constant for the formation (or more likely, a decrease in that of unfolding) of that intermediate. At the same time, however, a decrease in cooperativity makes it difficult to know what to compare between the mutant and the wild-type. For a highly cooperative denaturation, one can set the difference between the midpoint of the denaturation curve and the final denaturant concentration to be equal for comparative purposes. For noncooperative denaturation, there is no simple way to compare the rate constants for folding or unfolding in the mutant to those of the wild-type protein.

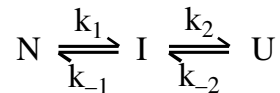
Another criterion is the slope of the chevron plot—i.e., how the rate constant changes as a function of the final denaturant concentration (ignoring effects of proline isomerization and off-pathway forms). The rate constant as a function of denaturant concentration is frequently defined as:

$$\ln k = \ln k_0 -/+ (m/RT)[D]$$

where  $k_0$  is the rate constant in the absence of denaturant,  $m$  is related to extent of cooperativity in the equilibrium denaturation curve as mentioned here,  $D$  is the denaturant concentration, and the  $-/+$  indicates whether the rate constant examined is for folding or unfolding. Thus, a plot of  $\ln k$  as a function of denaturant concentration (at constant temperature) should have a slope directly proportional to  $-m$  (or  $m$  in the unfolding direction). If the equilibrium denaturation curve is asymmetric, the value of  $m$  may be different in the folding and unfolding directions. Thus, in theory, the slope and the cooperativity are directly correlated. It is important to remember, however, that these rate constants are apparent values, and include the microscopic rate constants of all the steps in the process. For a simple reversible process:



the observed rate constant is  $k_1 + k_{-1}$ . For the process:



two apparent rate constants,  $\tau_1$  and  $\tau_2$ , may be observed. In this case the observed rates are (approximately) related to the microscopic rate constants by the relationships  $\tau_1 = k_1 + k_{-1} + k_2 + k_{-2}$  and  $\tau_2 = [k_1(k_{-2} + k_2) + k_{-1}k_{-2}] / (k_1 + k_{-1} + k_2 + k_{-2})$ , respectively. For extreme dilutions of the denaturant (in the refolding direction) these may simplify to  $k_1 + k_2$  and  $[k_1k_2] / (k_1 + k_2)$  and if  $k_2 \ll k_1$ , then the apparent constants become the microscopic constants. It is not surprising that experimental values frequently deviate from theory for systems that exhibit several phases.

#### 4. Rate Measurements: Experimental Procedures

Whether using fluorescence, absorbance, circular dichroism, or other similar techniques, most standard stopped-flow mixing devices have dead times on the order of 1–2 ms. Most proteins appear to form a collapsed state well within the first ms (the “burst” phase). Slower steps seem to be associated with the stabilization of the final structure. For example, based on stopped-flow  $^{19}\text{F}$  NMR data, the slow steps in the refolding of *E. coli* dihydrofolate reductase are stabilization of side chains near the protein surface (39–41). Similarly, mutations in one turn of the fatty-acid-binding protein allow formation of an intermediate without the final stabilizing step (11). Thus, combining these stopped-flow experiments with turn scanning may help define the role of turn formation in obtaining the final stable protein structure.

It is clearly important to explore the effect of mutations on early events. We have already discussed changes in the amplitude of a burst phase. A better method may be the use of faster mixing methods to determine changes in apparent rate constants that are hidden in the burst.

With the advent of experimental techniques that can measure half-times of folding processes faster than the usual 1-ms stopped-flow dead time, it should be possible to see whether mutations affect early steps in folding. The use of faster techniques has recently been reviewed by Callender et al. (42) and by Plaxco and Dobson (43,44). These new approaches for monitoring faster events use certain techniques with time resolution as fast as picoseconds. Perhaps the simplest of these is the continuous-flow method using capillary tubes, which allows mixing within 50–100 ns (45). Several studies have now used this method (46,47). Other techniques include laser-induced temperature-jump, laser photolysis, optical electron transfer, fluorescence correlation spectroscopy, or energy transfer and NMR.

Oas and colleagues (48–51) have used dynamic NMR to investigate simple two-state systems by extrapolating observed rate constants back to zero denaturant concentrations to obtain values for rapid steps in the ns range for the refolding process. Native-state amide proton exchange has been used by Arrington and Robertson (52) with ovomucoid third domain to determine rates of folding and unfolding in the ns range. Gilmanishin et al. (53) have used temperature-jump (10-ns, laser-induced) and time-resolved IR spectroscopy in native apomyoglobin, and observed two relaxation phases with relaxation times of 48 ns and 132 ns. They attributed these to formation of substructures primarily related to helices. The slower of the two phases is attributed to tertiary interactions and desolvation of the helix, but the data are consistent with substructures guiding the folding process and with these substructures being independently formed. Ballew et al. (54) also used temperature-jump with this protein, and noted that the earliest steps during folding to a compact state were complete within 20 ns. Nolting et al. (55) have also used temperature-jump methods on the cold denatured mutant of barstar to obtain relaxation rates in the ns range. In a later article, Nolting et al. (56) examined the folding pathway over a time range from ns to s again using fluorescence changes as measured by temperature-jump techniques to examine the early times. Their data are consistent with a nucleation-condensation mechanism.

For the most part, however, these techniques have not been applied to systems in which there are mutations, especially where those mutations are in turns. As these methods become more available, such experiments will hopefully be done.

## 5. Experimental Approach to Selecting Mutations

Certainly there are no general rules for deciding what mutations to make in a given turn. As discussed in this chapter, from both an experimental and theoretical point of view, substitutions between glycine and other residues or between proline and other residues are the most obvious choices. Hutchinson and Thornton (57) have presented extensive data for sequence preferences in different  $\alpha$ -turn types that could be useful in deciding what mutation to make. Aside from glycine and proline changes, one should consider other steric or hydrogen-bonding effects. Substitution of a  $\beta$ -branched chain amino acid for one that has  $\phi, \psi$  angles in a nonallowed region will certainly change the turn type, as will almost any substitution of a glycine. Substitutions between hydrophobic and hydrophilic residues may alter the solvent accessibility of the turn. While positions 2 and 3 of a  $\beta$ -turn are obvious candidates for substitution, residues adjacent to the turn—especially those that may affect packing within the turn—should be considered. Random mutagenesis of the two residues in the turn could be useful, but with the wide range of possible mutant proteins, a screen for function may be necessary.

## 6. Computational Studies: Theory for Turn Folding and Structure

Over the past decade, molecular dynamics and other simulation techniques have been used to explore the structural propensities and conformational dynamics of a variety of short turn-like peptide sequences. Advances in force-field accuracy and available computer power now allow simulation to serve as a viable complement of experiment. Indeed, because of the all-atom level of detail provided

by simulation, it could eventually become a preferred method for interpreting and correlating more ambiguous structural results. For example, reliable theoretical estimation of conformational population densities would greatly aid the interpretation of ambiguous NMR data for flexible peptides. Steps toward this ultimate goal are already underway.

Molecular dynamics simulation of turn peptides with explicit representation of solvent is still limited to the ns to ms time-scale. Fortunately, many of these sequences adopt relatively self-contained structures within full proteins, and are usually devoid of large, energetic barriers to conformational interconversion. Thus, even ns-scale MD simulations can expose some of the structural variability and dynamic behavior of turns. Two early reviews of peptide simulations (58,59) provide an excellent survey of this field through 1993. Here, we present an update and attempt to infer some general principles regarding the behavior of turns in protein structure.

In early work, Tobias et al. (60) used umbrella sampling methods to explore the free-energy surfaces of the blocked dipeptides Ac-Ala-Ala-NMe and Ac-Pro-Ala-NMe in aqueous solution. Based on calculated equilibrium constants for unfolding of type I turn structure, they found that the extended conformations were favored for both peptides by 5 to 10 kcal/mol. Additional studies with glycine replacing alanine in the second position suggested that glycine destabilizes the extended states, but the manifold of type I turn structures still lies 3 kcal/mol higher in free energy (58). Further simulations of the stability of type II turns suggest that Ac-Ala-Gly-NMe may be marginally stable as a type II turn. All other sequences again favor the extended form. The Ala-Gly result is corroborated by independent simulations from a second group (61).

Molecular orbital results at the HF/6-31G\* level also predicted that the extended forms of capped Gly-Gly and Ala-Ala are enthalpically favored over type I and II turns by values in the 1–9 kcal/mol range (62). Type I and II structures are even less favorable for these sequences. As expected, inclusion of electron correlation at the MP2 level favors the hydrogen-bonded turn forms. However, the authors

claim that correlation energy effects and intramolecular entropic terms compensate so that the HF energies are a fair approximation to the true enthalpy differences. *Ab initio* MO calculations coupled with the PCM solvation model (62), MD with explicit solvent, and finite-difference Poisson-Boltzmann calculations with the MEAD package (63) all agree that solvation effects favor type I over type II turns for all combinations of amino acids at positions 2 and 3 of a  $\beta$ -turn. Decomposition of the free-energy difference between extended and turn conformations indicates that peptide-water entropy is the major term favoring extended structures. Finally, Monte Carlo sampling of a variety of blocked dipeptides using the CHARMM19 force field plus Poisson-Boltzmann solvation (64) again finds the extended form to be favored over turn types I, I', II and II' by 1.6 to 7.7 kcal/mol depending on the sequence. However, with the exception of Gly-Gly, the most stable turn type for each sequence was found to be the one most commonly observed in protein structures. The Gly-Gly occurs frequently in type I turns of  $\beta$ -hairpins where the strand twist is apparently able to overcome local energetic effects.

Thus, both force-field and quantum mechanical results for these small peptides lead to the conclusion that reverse turns are intrinsically unstable in the absence of side-chain interactions and the tertiary protein environment.

Do turn types interconvert? Reaction path calculations on a capped Ala tripeptide as a model reverse-turn sequence (65) find only low barriers between extended and turn-like conformations. Interconversion pathways tend to involve sequential rotation about single backbone dihedral angles. This is in agreement with further path calculations performed using the CHARMM force field on an analog of the Ala tetrapeptide (66). Work with other force fields (Hart, R. K., Pappu, R. V., and Ponder, J. W., unpublished), semi-empirical quantum mechanics and detailed analysis of protein crystal structures (67) also suggest low barriers for interconversion, but find pathways involving concerted dihedral angle rotations. For example, the MOPAC results of Gunasekaran et al. (67) assign an

enthalpic barrier of only 3 kcal/mol to the concerted peptide bond flip needed to convert type II and type I  $\beta$ -turns. In summary, theory suggests interconversion between turn types, and between turn and nonturn structure, is energetically accessible, and may play an important role in peptide and protein dynamics.

## 7. Importance of Side-Chain Packing: The Type VI Turn

We indicated earlier that logical candidates for mutations in turns are either removal or insertion of glycine or proline. We now examine why, based on computational studies, the incorporation of a proline residue into position 3 of a turn may affect stability and/or kinetic properties. A well-studied example of a stable turn peptide containing proline is the Ser-Tyr-Pro-Phe-Asp-Val sequence, which adopts a type VI turn structure. NMR analysis finds a 70% population of type VIa and VIb turns in aqueous solution (68). A theoretical study of this same peptide using locally enhanced sampling (LES) methods reaches generally similar conclusions (69). These workers also find a type VI turn structure to be the preferred conformation. Their simulations suggest a possible kinetic pathway for the folding in this peptide family. First, electrostatic interactions involving the N- and C-termini and aspartate residue tend to enforce an end-to-end distance consistent with turn formation. Next, the backbone angles of the peptide rearrange in concert with a generalized hydrophobic collapse involving side chains. Finally, the hydrophobic residues pack into the characteristic type VI turn. This work also uncovers some potential “trapped” states containing *trans*-Pro residues. Molecules with the *trans*-linkage remain disordered with large end-to-end distances, and are not stabilized by hydrophobic interactions.

An independent study of the related Ala-Tyr-*cis*-Pro-Tyr-Asp-NMe sequence uncovered similar hairpin stabilizing factors. In contrast to the simulation results described for generic sequences, this peptide is stable as a turn structure during lengthy MD simulations. A 20-ns trajectory starting from an NMR-derived type VIa structure

makes three transitions between type VIa and VIb turns, but does not explore extended conformations (70). A further simulation, starting from an unfolded structure, folds to a compact turn structure within 2.7 ns. Finally, a 4.7-ns simulation starting from a nontype VI *cis*-Pro conformation is trapped in an unfolded state, which is stable over the course of the trajectory. Subsequently, a potential of mean force (PMF) constructed from the AMBER/OPLS energy function plus macroscopic solvation terms was used to select low-energy conformers from a random search (71). The PMF selected a structure similar to the NMR model as the lowest energy conformer. Inclusion of entropy estimates led to a final  $G_{\text{folding}}$  in the range  $-1.0$  to  $-2.1$  kcal/mol. These values are somewhat more favorable to turn formation than the NMR studies, perhaps because of incomplete sampling of the manifold of unfolded states.

Two factors indicate why is this particular type VI turn sequence is stable in a compact turn-like conformation. First, the proline residue at turn position 3 favors a *cis*-dihedral angle at the preceding peptide bond. The relative advantage is approx 2.6 kcal/mol over the *trans*-peptide bond favored for other amino acids (72). Equally or more important for this sequence is the packing of the two aromatic tyrosine residues against the proline ring in the type VI turn structure. In fact, the PMF calculations indicate that intrapeptide enthalpic interactions comprise the major term favoring the folded form, while polar solvation effects favor extended conformations.

Other theoretical work from Pettitt's group (73) examined the conformation of the tetrapeptide tuftsin, Thr-Lys-Pro-Arg, in water and in 1 M NaCl solution. In this case, the experimental NMR results less conclusively favor a type VI turn, and a separate series of simulations was used to study the *cis*- and *trans*-proline structures. Again, the *cis*-conformers tended to adopt compact conformations which are fairly rigid by typical peptide standards. The lysine and arginine side chains both tended to form intramolecular hydrogen bonds to the peptide backbone in water. The presence of salt had relatively little effect on the backbone structure, but did alter the



average side-chain orientations. The *trans*-tuftsin simulation is dominated by more extended conformations.

## 8. Turns in $\beta$ -Hairpin Structures

Several simulations show initial hydrophobic collapse followed by formation of turn structure, coupled in concert with detailed packing interactions. An early MD study (74) of the temperature unfolding of the residue 85-102  $\beta$ -hairpin from barnase reported all-atom simulations from the native structure at 300 K, 450 K, and 600 K. The isolated hairpin in aqueous solution was stable over the course of 300 psec at 300 K, with an average r.m.s. from native of about 0.8Å for backbone atoms. Comparison of fluctuations in torsional angles during the 300 K hairpin simulation with those from a similar simulation of the full protein showed similar flexibility for the backbone angles. However, rotation about side-chain bonds was much more restricted in the full protein than in the isolated hairpin. Three persistent hydrogen bonds during the simulation involve the amide hydrogens of residues which are the most protected amide hydrogens during NMR hydrogen-exchange experiments. Following equilibration at 450 K, the structure is characterized by loss of hydrogen bonds at the extremities of the hairpin, more frequent exchange of hydrogen bonds with water, volume expansion, and formation of a large hydrophobic side-chain cluster containing both native and nonnative contacts. This loosely packed, yet still compact state was stable for the entire simulation 300 psec at 450 K, and for 150 psec at 600 K. Overall, the simulation data correlates well with current ideas generated from an experimental study of barnase unfolding.

In a recent report, Sung (75) used Monte Carlo sampling with a simple all-atom potential containing dielectric screened electrostatics and a surface area-based hydrophobic effect term to fold a capped poly-Val 12-mer with glycine substituted at the two central positions. Once again, the folding proceeded through an initial gen-

eralized collapse to a compact U-shaped structure as mediated by the hydrophobic effect. This same potential folds poly-Ala based sequences, which lack the potential for large hydrophobic stabilization, into  $\alpha$ -helical motifs.

Many theories seem to favor a folding path directed by hydrophobic stabilization in which the turn does not need to be favorable or particularly stabilizing, but merely accessible and not prohibited. Recent thermodynamic decomposition of the experimental data shows hairpin folding to be an endothermic, entropy-driven process with a large negative  $C_p$ , characteristic of a pathway dominated by formation of a hydrophobic core instead of specific enthalpically stabilized conformational preferences (76). Simulations of small regions of proteins using LINUS (77), however, suggest that folding is hierarchical and that there are biases towards local structures such as  $\alpha$ -hairpins and  $\alpha$ -turns primarily established by steric effects and hydrogen bonds and enhanced by hydrophobic interactions (78).

It is also likely that the situation is qualitatively different in larger globular protein systems. For example, Scheinerman and Brooks (79) have studied the free energy of folding of the 56-residue B1 segment of *Streptococcal* protein G along a reaction coordinate characterized by the percentage of native contacts. This globular domain is topologically similar to the much-studied chymotrypsin inhibitor 2 (CI2), and contains two  $\alpha$ -hairpins separated in the primary sequence by an  $\alpha$ -helical region. While the helix generally forms before the sheet structure, these researchers found that the earliest structure formed consisted of the N-terminus of the helix and the turn of the second hairpin. These two regions pack against each other in the native structure, and seem to independently form nucleation sites for the folding process.

## 9. Turns in Helix-Turn-Helix Structures

Sung and Wu (80) have used simulation to model the deformation of a long helix into various distorted helix-turn-helix conformations. The transition between the two forms occurs on a much longer time scale than simple helix propagation. A small model pep-

tion similar to the central helix-turn-helix portion of ROP was folded using Monte Carlo dynamics (81). In the latter study, four of six trajectories ended in stable native-like conformations. The folding showed relatively fast formation of two helical regions of unequal length, followed by dynamic behavior in accord with the Karplus and Weaver diffusion-collision model. Only in this latter stage did the sharp reverse turn develop, initiated by the formation of hydrophobic contacts at the end of the shorter helix. Once the two helices come into direct contact, the turn region expands by annexing some glycine residues from the last helical turn of the longer helix. In the final stable structure, the two helices are of nearly equal length. Both of these simulation studies are consistent with flexibility in the turn residues during the early stages of the folding event, with stable turn formation only after the helices are fully formed. They are also consistent with the experimental data discussed earlier.

## Conclusion

There is no simple answer to the question posed at the beginning of this chapter. Computational studies reveal that small peptides which reflect turn motifs sample many conformational states, including those that ultimately appear in the final native structure. They also suggest that mutations in turn residues will certainly bias the amount of time spent in a particular local structure, and therefore the kinetic folding rates. Experimental evidence clearly shows that changes in turns or turn structures can affect both thermodynamic stability and kinetic properties. In addition to the turn itself, longer-range interactions between residues surrounding the turn are clearly important. It is surprising how few systematic experimental kinetic measurements have been made of the consequences of mutations in turns. Mutations that either include or replace glycine or proline residues may be particularly useful in this regard, but substitution between hydrophobic and hydrophilic residues or between those with different size side chains may be equally useful. One important result of such studies may be the possibility of creating long-lived intermediates. We propose turn scanning as a general

method to quantitatively examine the importance of turns in the mechanism of protein folding with the understanding that such studies also require the concomitant use of biophysical techniques including theoretical simulation.

## Acknowledgments

This work was supported by NIH Grant DK13332 (to Carl Frieden) and a Jane Coffin Childs Fellowship (to Enoch Huang).

## References

1. Anfinsen, C. B., Haber, M., Sela, M., and Jr., W. F. H. (1961) The kinetics of formation of native ribonuclease during oxidation of the reduced polypeptide chain. *Proc. Natl. Acad. Sci. USA* **47**, 1309–1314.
2. Richardson, J. S. (1981) The anatomy and taxonomy of protein structure. *Adv. Protein Chem.* **34**, 167–339.
3. Rose, G. D., Gierasch, L. M., and Smith, J. A. (1985) Turns in peptides and proteins. *Adv. Protein Chem.* **37**, 1–109.
4. Fasman, G. D. (1989) Protein conformational prediction. *Trends Biochem. Sci.* **14**, 295–299.
5. Wright, P. E., Dyson, H. J., and Lerner, R. A. (1988) Conformation of peptide fragments of proteins in aqueous solution: implications for initiation of protein folding. *Biochemistry* **27**, 7167–7175.
6. Finkelstein, A. V. (1991) Rate of beta-structure formation in polypeptides. *Proteins* **9**, 23–27.
7. Blanco, F. J., Rivas, G., and Serrano, L. (1994) A short linear peptide that folds into a native stable beta-hairpin in aqueous solution. *Nat. Struct. Biol.* **1**, 584–590.
8. Yang, A. S., Hitz, B., and Honig, B. (1996) Free energy determinants of secondary structure formation. 3. Beta-turns and their role in protein folding. *J. Mol. Biol.* **259**, 873–882.
9. Schonbrunner, N., Koller, K. P., and Kiefhaber, T. (1997) Folding of the disulfide-bonded beta-sheet protein tendamistat—rapid two-state folding without hydrophobic collapse. *J. Mol. Biol.* **268**, 526–538.
10. Baldwin, R. L. and Rose, G. D. (1999) Is protein folding hierarchic? II. Folding intermediates and transition states. *Trends Biochem. Sci.* **24**, 77–83.

11. Kim, K., Ramanathan, R., and Frieden, C. (1997) Intestinal fatty acid binding protein: a specific residue in one turn appears to stabilize the native structure and be responsible for slow refolding. *Protein Sci.* **6**, 364–372.
12. Zhou, H. X., Hoess, R. H., and DeGrado, W. F. (1996) In vitro evolution of thermodynamically stable turns. *Nat. Struct. Biol.* **3**, 446–451.
13. de Alba, E., Jimenez, M. A., and Rico, M. (1997) Turn residue sequence determines  $\beta$ -hairpin conformation in designed peptides. *J. Am. Chem. Soc.* **119**, 175–183.
14. Munoz, V., Thompson, P. A., Hofrichter, J., and Eaton, W. A. (1997) Folding dynamics and mechanism of beta-hairpin formation. *Nature* **390**, 196–199.
15. Munoz, V., Henry, E. R., Hofrichter, J., and Eaton, W. A. (1998) A statistical mechanical model for beta-hairpin kinetics. *Proc. Natl. Acad. Sci. USA* **95**, 5872–5879.
16. Blanco, F. J. and Serrano, L. (1995) Folding of protein G B1 domain studied by the conformational characterization of fragments comprising its secondary structure elements. *Eur. J. Biochem.* **230**, 634–649.
17. Ramirez-Alvarado, M., Blanco, F. J., and Serrano, L. (1996) De novo design and structural analysis of a model beta-hairpin peptide system. *Nat. Struct. Biol.* **3**, 604–612.
18. Ramirez-Alvarado, M., Blanco, F. J., Niemann, H., and Serrano, L. (1997) Role of beta-turn residues in beta-hairpin formation and stability in designed peptides. *J. Mol. Biol.* **273**, 898–912.
19. Blanco, F., Ramirez-Alvarado, M., and Serrano, L. (1998) Formation and stability of beta-hairpin structures in polypeptides. *Curr. Opin. Struct. Biol.* **8**, 107–111.
20. Schaefer, M., Bartels, C., and Karplus, M. (1998) Solution conformations and thermodynamics of structured peptides: molecular dynamics simulation with an implicit solvation model. *J. Mol. Biol.* **284**, 835–848.
21. Kim, K. and Frieden, C. (1998) Turn scanning by site-directed mutagenesis: Application to the protein folding problem using the intestinal fatty acid binding protein. *Protein Sci.* **7**, 1821–1828.
22. Ybe, J. A. and Hecht, M. H. (1996) Sequence replacements in the central beta-turn of plastocyanin. *Protein Sci.* **5**, 814–824.
23. Gu, H., Kim, D., and Baker, D. (1997) Contrasting roles for symmetrically disposed beta-turns in the folding of a small protein. *J. Mol. Biol.* **274**, 588–596.

24. Brunet, A. P., Huang, E. S., Huffine, M. E., Loeb, J. E., Weltman, R. J., and Hecht, M. H. (1993) The role of turns in the structure of an alpha-helical protein. *Nature* **364**, 355–358.
25. Predki, P. F., Agrawal, V., Brunger, A. T., and Regan, L. (1996) Amino-acid substitutions in a surface turn modulate protein stability. *Nat. Struct. Biol.* **3**, 54–58.
26. Castagnoli, L., Ve triani, C., and Cesareni, G. (1994) Linking an easily detectable phenotype to the folding of a common structural motif. Selection of rare turn mutations that prevent the folding of Rop. *J. Mol. Biol.* **237**, 378–387.
27. Peters, K., Hinz, H. J., and Cesareni, G. (1997) Introduction of a proline residue into position 31 of the loop of the dimeric 4-alpha-helical protein Rop causes a drastic destabilization. *Biol. Chem.* **378**, 1141–1152.
28. MacBeath, G., Kast, P., and Hilvert, D. (1998) Exploring sequence constraints on an interhelical turn using in vivo selection for catalytic activity. *Protein Sci.* **7**, 325–335.
29. Nagi, A. D., Anderson, K. S., and Regan, L. (1999) Using loop length variants to dissect the folding pathway of a four-helix-bundle protein. *J. Mol. Biol.* **286**, 257–265.
30. Viguera, A. R., and Serrano, L. (1997) Loop length, intramolecular diffusion and protein folding. *Nat. Struct. Biol.* **4**, 939–946.
31. Ladurner, A. G. and Fersht, A. R. (1997) Glutamine, alanine or glycine repeats inserted into the loop of a protein have minimal effects on stability and folding rates. *J. Mol. Biol.* **273**, 330–337.
32. Nagi, A. D. and Regan, L. (1997) An inverse correlation between loop length and stability in a four-helix-bundle protein. *Fold. Des.* **2**, 67–75.
33. Helms, L. R. and Wetzel, R. (1995) Destabilizing loop swaps in the CDRs of an immunoglobulin VL domain. *Protein Sci.* **4**, 2073–2081.
34. Jackson, S. E. and Fersht, A. R. (1991) Folding of chymotrypsin inhibitor 2. 1. Evidence for a two-state transition. *Biochemistry* **30**, 10,428–10,435.
35. Fersht, A. R., Matouschek, A., and Serrano, L. (1992) The folding of an enzyme. I. Theory of protein engineering analysis of stability and pathway of protein folding. *J. Mol. Biol.* **224**, 771–782.
36. Baldwin, R. L. (1996) On-pathway versus off-pathway folding intermediates. *Fold. Des.* **1**, R1–R8.
37. Otzen, D. E., Kristensen, O., Proctor, M., and Oliveberg, M. (1999) Structural changes in the transition state of protein folding: alterna-

- tive interpretations of curved chevron plots. *Biochemistry* **38**, 6499–6511.
38. Santoro, M. M. and Bolen, D. W. (1988) Unfolding free energy changes determined by the linear extrapolation method. 1. Unfolding of phenylmethanesulfonyl alpha-chymotrypsin using different denaturants. *Biochemistry* **27**, 8063–8068.
  39. Hoeltzli, S. D. and Frieden, C. (1995) Stopped-flow nmr spectroscopy—real-time unfolding studies of 6-<sup>19</sup>F-tryptophan-labeled escherichia coli dihydrofolate reductase. *Proc. Natl. Acad. Sci. USA* **92**, 9318–9322.
  40. Hoeltzli, S. D. and Frieden, C. (1994) <sup>19</sup>F NMR spectroscopy of [6-<sup>19</sup>F]tryptophan-labeled E. coli dihydrofolate reductase: equilibrium folding and ligand binding studies. *Biochemistry* **33**, 5502–5509.
  41. Hoeltzli, S. D. and Frieden, C. (1998) Refolding of [6-F-<sup>19</sup>] tryptophan-labeled Escherichia coli dihydrofolate reductase in the presence of ligand—a stopped-flow NMR spectroscopy study. *Biochemistry* **37**, 387–398.
  42. Callender, R. H., Dyer, R. B., Gilmanshin, R., and Woodruff, W. H. (1998) Fast events in protein folding: the time evolution of the primary process. *Ann. Rev. Phys. Chem.* **49**, 173–202.
  43. Plaxco, K. W. and Dobson, C. M. (1996) Time-resolved biophysical methods in the study of protein folding. *Curr. Opin. Struct. Biol.* **6**, 630–636.
  44. Plaxco, K. W. and Dobson, C. M. (1998) Monitoring protein folding using time-resolved biophysical techniques, in *Protein Dynamics, Function and Design* (Jardetzky, O. and Lefevre, J., eds.), Plenum Press.
  45. Takahashi, S., Yeh, S. R., Das, T. K., Chan, C. K., Gottfried, D. S., and Rousseau, D. L. (1997) Folding of cytochrome c initiated by submillisecond mixing. *Nat. Struct. Biol.* **4**, 44–50.
  46. Shastry, M. C., Luck, S. D., and Roder, H. (1998) A continuous-flow capillary mixing method to monitor reactions on the microsecond time scale. *Biophys. J.* **74**, 2714–2721.
  47. Chan, C. K., Hu, Y., Takahashi, S., Rousseau, D. L., Eaton, W. A., and Hofrichter, J. (1997) Submillisecond protein folding kinetics studied by ultrarapid mixing. *Proc. Natl. Acad. Sci. USA* **94**, 1779–1784.
  48. Huang, G. S. and Oas, T. G. (1995) Submillisecond folding of monomeric lambda repressor. *Proc. Natl. Acad. Sci. USA* **92**, 6878–6882.

49. Burton, R. E., Huang, G. S., Daugherty, M. A., Fullbright, P. W., and Oas, T. G. (1996) Microsecond protein folding through a compact transition state. *J. Mol. Biol.* **263**, 311–322.
50. Burton, R. E., Huang, G. S., Daugherty, M. A., Calderone, T. L., and Oas, T. G. (1997) The energy landscape of a fast-folding protein mapped by ala-gly substitutions. *Nat. Struct. Biol.* **4**, 305–310.
51. Burton, R. E., Myers, J. K., and Oas, T. G. (1998) Protein folding dynamics: quantitative comparison between theory and experiment. *Biochemistry* **37**, 5337–5343.
52. Arrington, C. B. and Robertson, A. D. (1997) Microsecond protein folding kinetics from native-state hydrogen exchange. *Biochemistry* **36**, 8686–8691.
53. Gilmanshin, R., Williams, S., Callender, R. H., Woodruff, W. H., and Dyer, R. B. (1997) Fast events in protein folding—relaxation dynamics of secondary and tertiary structure in native apomyoglobin. *Proc. Natl. Acad. Sci. USA* **94**, 3709–3713.
54. Ballew, R. M., Sabelko, J., and Gruebele, M. (1996) Direct observation of fast protein folding—the initial collapse of apomyoglobin. *Proc. Natl. Acad. Sci. USA* **93**, 5759–5764.
55. Nolting, B., Golbik, R., and Fersht, A. R. (1995) Submillisecond events in protein folding. *Proc. Natl. Acad. Sci. USA* **92**, 10,668–10,672.
56. Nolting, B., Golbik, R., Neira, J. L., Solergonzalez, A. S., Schreiber, G., and Fersht, A. R. (1997) The folding pathway of a protein at high resolution from microseconds to seconds. *Proc. Natl. Acad. Sci. USA* **94**, 826–830.
57. Hutchinson, E. G. and Thornton, J. M. (1994) A revised set of potentials for beta-turn formation in proteins. *Protein Sci.* **3**, 2207–2216.
58. Brooks, C. L. and Case, D. A. (1993) Simulations of peptide conformational dynamics and thermodynamics. *Chem. Rev.* **93**, 2487–2502.
59. Hermans, J. (1993) Molecular dynamics simulations of helix and turn propensities in model peptides. *Curr. Opin. Struct. Biol.* **3**, 270–276.
60. Tobias, D. J., Mertz, J. E., and Brooks, C. L. (1991) Nanosecond time scale folding dynamics of a pentapeptide in water. *Biochemistry* **30**, 6054–6058.
61. Hermans, J. and Anderson, A. G. (1990) Microfolding: use of molecular dynamics simulations to assess conformational stability of folded peptides and proteins in relation to protein engineering, in *Crystallographic and Modeling Methods in Molecular Design* (Bugg, C. and Ealick, S., eds.), Springer-Verlag, New York, NY, pp. 95–113.



62. Möhle, K., Gußmann, M., and H.-J., H. (1997) Structural and energetic relations between turns. *J. Comput. Chem.* **18**, 1415–1430
63. Ösapay, K., Young, W. S., Bashford, D., Brooks, C. L., and Case, D. A. (1996) Dielectric continuum models for hydration effects on peptide conformational transitions. *J. Phys. Chem.* **100**, 2698–2705.
64. Yang, A. S., Hitz, B., and Honig, B. (1996) Free energy determinants of secondary structure formation: III. beta-turns and their role in protein folding. *J. Mol. Biol.* **259**, 873–882.
65. Lazaridis, T., Tobias, D. J., Brooks, C. L., and Paulaitis, M. E. (1991) Reaction paths and free-energy profiles for conformational transitions—an internal coordinate approach. *J. Chem. Phys.* **95**, 7612–7625.
66. Czerminski, R. and Elber, R. (1989) Reaction path study of conformational transitions and helix formation in a tetrapeptide. *Proc. Natl. Acad. Sci. USA* **86**, 6963–6967.
67. Gunasekaran, K., Gomathi, L., Ramakrishnan, C., Chandrasekhar, J., and Balaram, P. (1998) Conformational interconversions in peptide beta-turns: analysis of turns in proteins and computational estimates of barriers. *J. Mol. Biol.* **284**, 1505–1516.
68. Yao, J., Dyson, H. J., and Wright, P. E. (1994) Three-dimensional structure of a type VI turn in a linear peptide in water solution. Evidence for stacking of aromatic rings as a major stabilizing factor. *J. Mol. Biol.* **243**, 754–766.
69. Mohanty, D., Elber, R., Thirumalai, D., Beglov, D., and Roux, B. (1997) Kinetics of peptide folding: computer simulations of SYPFDV and peptide variants in water. *J. Mol. Biol.* **272**, 423–442.
70. Demchuk, E., Bashford, D., and Case, D. A. (1997) Dynamics of a type VI reverse turn in a linear peptide in aqueous solution. *Fold. Des.* **2**, 35–46.
71. Demchuk, E., Bashford, D., Gippert, G. P., and Case, D. A. (1997) Thermodynamics of a reverse turn motif. Solvent effects and side-chain packing. *J. Mol. Biol.* **270**, 305–317.
72. Jorgensen, W. L. and Gao, J. (1988) Cis-trans energy difference for the peptide bond in the gas phase and in aqueous solution. *J. Am. Chem. Soc.* **110**, 4212–4216.
73. Valdeavella, C. V., Blatt, H. D., and Pettitt, B. M. (1995) Simulations of conformers of tuftsin and a cyclic tuftsin analog. *Int. J. Pept. Protein Res.* **46**, 372–380.
74. Pugliese, L., Prevost, M., and Wodak, S. J. (1995) Unfolding simulations of the 85-102 beta-hairpin of barnase. *J. Mol. Biol.* **251**, 432–447.

75. Sung, S. S. (1999) Monte Carlo simulations of beta-hairpin folding at constant temperature. *Biophys. J.* **76**, 164–175.
76. Maynard, A. J., Sharman, G. J., and Searle, M. S. (1998) Origin of b-hairpin stability in solution: structural and thermodynamic analysis of the folding of a model peptide supports hydrophobic stabilization in water. *J. Am. Chem. Soc.* **120**, 1996–2007.
77. Srinivasan, R. and Rose, G. D. (1995) LINUS: a hierarchic procedure to predict the fold of a protein. *Proteins* **22**, 81–99.
78. Baldwin, R. L. and Rose, G. D. (1999) Is protein folding hierarchic? I. Local structure and peptide folding. *Trends Biochem. Sci.* **24**, 26–33.
79. Sheinerman, F. B. and Brooks, C. L., 3rd (1998) Calculations on folding of segment B1 of streptococcal protein G. *J. Mol. Biol.* **278**, 439–456.
80. Sung, S.-S. and Wu, X.-W. (1996) Molecular dynamics simulations of synthetic peptide folding. *Proteins* **25**, 202–214.
81. Hoffmann, D. and Knapp, E. W. (1997) Folding pathways of a helix-turn-helix model protein. *J. Phys. Chem. B* **101**, 6734–6740.